Princeton Plasma Physics Laboratory

PPPL- 4982

PPPL- 4982

Nonmodal Growth of the Magneto-rotational Instability

J. Squire and A. Bhattacharjee

JANUARY, 2014

PPPL PRINCETON PLASMA PHYSICS LABORATORY

Prepared for the U.S. Department of Energy under Contract DE-AC02-09CH11466.

Princeton Plasma Physics Laboratory
Report Disclaimers

Full Legal Disclaimer

Trademark Disclaimer

PPPL Report Availability

Princeton Plasma Physics Laboratory:

http://www.pppl.gov/techreports.cfm

Office of Scientific and Technical Information (OSTI):

http://www.osti.gov/bridge

Related Links:

U.S. Department of Energy

Office of Scientific and Technical Information

Fusion Links

Nonmodal growth of the magneto-rotational instability

J. Squire[1] and A. Bhattacharjee[1,2]

[1]*Department of Astrophysical Sciences and Princeton Plasma Physics Laboratory, Princeton University, Princeton, NJ 08543*

[2]*Max Planck/Princeton Center for Plasma Physics, Princeton University, Princeton, NJ 08543*

(Dated: January 16, 2014)

Abstract

We analyze the linear growth of the magneto-rotational instability (MRI) in the short time limit using nonmodal methods. Our findings are quite different to standard results, illustrating that shearing wave energy can grow at the maximum MRI rate, $-d\Omega/d\ln r$, for *any* choice of azimuthal and vertical wavelengths. In addition, by comparing the growth of shearing waves with static eigenmode-like structures, we show that over short time-scales shearing waves will always be dynamically more important than static structures in the ideal limit. By demonstrating that some fast linear growth is possible at all wavelengths, these results suggest that nonmodal linear physics could play a fundamental role in MRI turbulence.

Since the seminal work of Balbus and Hawley [1], the magneto-rotational instability (MRI) has emerged as promising explanation for the observed momentum transport in accretion disks. In particular, the nonlinear development of the instability has been shown to lead to sustained turbulence and dynamo action in both local shearing box (*e.g.,* [2–4]) and global (*e.g.,* [5]) nonlinear simulations. Despite substantial concern about transport convergence with dissipation parameters [6, 7] it seems that such results are relatively robust [4], persisting both with and without an imposed magnetic field and somewhat independently of boundary conditions and background density profiles [3]. Nonetheless, even in the simplest local case, a thorough understanding of the nature of the turbulence and the dynamo mechanism is lacking (see, for instance [8]). Several promising closure models and dynamo ideas (*e.g.,* [9–12]) require further testing, and there has been less work on the nature of the turbulent cascade [13] (if it even exists in the usual sense [14]). The relevance of linear eigenmodes in these processes seems to have mostly been discounted (*e.g.,* [7]), although there have been hints that linear shearing waves have substantial dynamical importance [10, 12].

The study of the linear eigenmodes of a system is, in the most basic sense, an attempt to answer the following question: How much can the system grow in time and what initial conditions will maximize this growth? If said system is self-adjoint in a physically relevant norm, the eigenspectrum is certainly the best way to approach this problem; initializing with the most unstable eigenmode will maximize growth of the disturbance at all times. However, the question becomes more complex if the linear operator is not self-adjoint and *nonmodal* effects become important [15]. In particular, the answer can depend enormously on the time at which one wishes to maximize the growth, and the eigenvalue result is correct only in the limit $t \to \infty$. If one studies growth over shorter times, not only can growth rates be very much larger than predicted with eigenvalue analysis, but the most relevant structures can look very different to the eigenmodes. Investigations in this vein have been particularly fruitful in fluid dynamics, where they have cleanly answered longstanding questions about subcritical transition to turbulence in spectrally stable systems [16].

In this letter we approach the linear stability of the MRI from the nonmodal standpoint, studying the *short time* growth of perturbations. The picture that emerges suggests that eigenmode and asymptotic shearing wave growth estimates can be quite misleading, since over shorter time-scales relevant to a turbulent situation the growth can be very different than in the long-time limit. In particular, we prove that shearing wave structures (we include the axisymmetric mode as a special case of this) always grow faster over short time-scales than static (eigenmode-like) structures so long

as dissipation is not too large, a result that also holds with the inclusion of certain global effects. In addition, for the local ideal case, we show that the short time energy growth rate has the *same* maximum value, $-d\Omega/d\ln r$, regardless of the vertical and azimuthal wavelengths. To reinforce the notion that one must be very cautious when relying on eigenmode analyses and dispersion relations for the MRI, we finish the letter with an example illustrating how eigenmode analysis might lead to incorrect conclusions about the relative importance of different mode numbers in an experimentally relevant regime.

The significance of transient growth for non-axisymmetric MRI has been recognized in many previous papers (*e.g.,* [17–20]), which have mainly focused on the transience brought about by the time-dependent spatial structure of shearing waves. Our considerations differ in several respects from those given previously.

1. Curiously, it is generally assumed that shearing waves are the most relevant structures in local inquiries, while most global studies consider static eigenmode structures (but see [18, 21]). We advocate that the dynamical relevance of each type of structure should be determined based on growth rates, since strongly amplified structures will dominate when starting from random initial conditions. With this in mind, we *prove* (within a WKB-like approximation) that in almost all regimes, shearing waves grow faster on short time-scales.

2. We find that the fastest short-time shearing wave growth occurs in a regime where standard analytic results (based on WKB eigenmodes [17, 19, 20]) are not valid.

3. We find that transient growth can be significant even for axisymmetric modes.

4. We argue that both shearing waves and eigenmodes can be important in many situations. While shearing waves invariably grow faster over moderate time-scales, they can transition into an eigenmode as the radial wavenumber becomes large and continue growing (if the eigenmode is unstable). In this way the eventual decay of shearing waves at finite diffusivity is not physically important, even without consideration of nonlinearities. This type of behavior is illustrated in Figs. 2 and 3.

Local Calculation. Our starting point for the local calculation is the incompressible nonlinear

MHD equations in the shearing box

$$\begin{aligned}
&\frac{\partial \boldsymbol{u}}{\partial t} + (\boldsymbol{u}\cdot\nabla)\,\boldsymbol{u} + 2\Omega\hat{\boldsymbol{z}}\times\boldsymbol{u} = -\nabla p + \nabla\times\boldsymbol{B}\times\boldsymbol{B} \\
&\qquad + 2q\Omega^2 x\hat{\boldsymbol{x}} - \nabla\Phi + \bar{\nu}\nabla^2\boldsymbol{u}, \\
&\frac{\partial \boldsymbol{B}}{\partial t} + (\boldsymbol{u}\cdot\nabla)\,\boldsymbol{B} = (\boldsymbol{B}\cdot\nabla)\,\boldsymbol{u} + \bar{\eta}\nabla^2\boldsymbol{b}, \\
&\quad \nabla\cdot\boldsymbol{u} = 0, \quad \nabla\cdot\boldsymbol{B} = 0.
\end{aligned} \tag{1}$$

Here, the directions x, y, z correspond respectively to the radial, azimuthal and vertical directions in the disk, Ω is the local rotation frequency and $q = -d\ln\Omega/d\ln r$ embodies the local velocity shear. We have used dimensionless variables normalized by the length scale L_0 and the time-scale $1/\Omega$ – as such $\Omega = 1$ in Eqs. (1). Since all parameters in our problem are of order 1, the fluid and magnetic diffusivities,$\bar{\nu}$ and $\bar{\eta}$, are the inverses of the fluid and magnetic Reynolds numbers respectively. The background velocity is taken to be azimuthal with linear shear in the radial direction, $\boldsymbol{u}_0 = -q\Omega x = -qx$, and the background magnetic field is taken to be constant, $\boldsymbol{B}_0 = \left(0, B_{0y}, B_{0z}\right)$. We linearize about this background and Fourier analyze in y and z, denoting the respective wave-numbers k_y and k_z. Changing to convenient Orr-Sommerfeld like variables [19], $u = u_x$, $B = B_x$, $\zeta = ik_z u_y - ik_y u_z$, $\eta = ik_z B_y - ik_y B_z$, we are left with 4 coupled partial differential equations in x and t.

The general idea of nonmodal growth calculations is to compute, for some chosen time, the initial conditions that lead to the maximum growth of the solution under the chosen norm. We use the energy of the perturbation, $E = \int d\boldsymbol{x}\left(|\boldsymbol{u}|^2 + |\boldsymbol{B}|^2\right)$, as the norm throughout this work, since it seems the most physically relevant choice [16]. For the sake of clarity, consider the general linear system $\partial U/\partial t = \mathcal{L}(t)U(t)$, with solution $U(t) = K(t)U(0)$. The maximum growth at t, $G(t) = \max_{U(0)} \|K(t)U(0)\|_E^2 \,/\, \|U(0)\|_E^2$ (where $\|\cdot\|_E$ denotes the energy norm), can be calculated by changing to the 2-norm using the Cholesky decomposition

$$\|U\|_E^2 = U^\dagger \cdot M_E(t) \cdot U = U^\dagger \cdot F^\dagger(t)F(t) \cdot U = \|F(t)U\|_2^2\,, \tag{2}$$

and computing the largest singular value of the matrix $F(t)K(t)F^{-1}(0)$. For the analytic results presented in this letter, we compute the growth rate at $t = 0^+$, $G^+_{max} = \max_{U(0)} \|U(t)\|_E^{-2} \frac{d}{dt}\|U(t)\|_E^2\Big|_{t=0^+}$. Note that for a self-adjoint system G^+_{max} is simply (twice) the most unstable eigenvalue growth.

Differentiating $K(t)$ and changing to the 2-norm, we obtain the result

$$G^{+}_{max} = \lambda_{max}\left(\Lambda + \Lambda^{\dagger}\right), \tag{3}$$

where $\Lambda = F\mathcal{L}F^{-1} + \partial_t F F^{-1}\big|_{t=0}$ and λ_{max} denotes the largest eigenvalue.

Our goal is compare the growth of shearing waves with that of static, eigenmode-like structures. We study this at a given x value using a WKB approximation. While caution is advised in attempting to predict stability using such methods [22], here we are simply comparing static and shearing growth at a *given* k_x. Thus, subtle issues regarding the choice of k_x relevant to an eigenmode are alleviated and we make no claim that these approximations are a substitute for the solution of the x dependent problem. The static equations can easily be derived to lowest order by inserting the WKB ansatz $f(x,t) \sim f(t)\, e^{ik_x x}$, and substituting $\frac{\partial}{\partial t} \rightarrow \frac{\partial}{\partial t} - i\boldsymbol{u}_0 k_y = \frac{\partial}{\partial t} + iqxk_y$ (this simply shifts the real part of the spectrum without changing growth rates). The shearing wave equations are exact [23] and are derived by inserting the ansatz $f(x,t) = f(t)\exp\left(iqk_y\,(t-t_0)\,x\right)$ for each independent variable. We obtain

$$\frac{\partial}{\partial t}U(t) = \begin{pmatrix} -\bar{\nu}k^2 - 2\Xi q k_x k_y/k^2 & -2ik_z/k^2 & iF & 0 \\ i(q-2)k_z & -k^2\bar{\nu} & 0 & iF \\ iF & 0 & -k^2\bar{\eta} & 0 \\ 0 & iF & -iqk_z & -k^2\bar{\eta} \end{pmatrix} \cdot U(t)\,. \tag{4}$$

where $\Xi = 0$ or 1 for static and shearing waves respectively, $F = k_y B_{0y} + k_z B_{0z}$, $k^2 = k_x^2 + k_y^2 + k_z^2$, $U(t) = (u, \zeta, B, \eta)$ and we have used $\Omega = 1$. For the shearing waves, the equations are time-dependent since $k_x = qk_y\,(t - t_0)$. Solving for the eigenvalues of Eqs. (4) with $k_x = k_y = 0$ leads to the standard MRI dispersion relation [1].

Converting the energy norm into (u, ζ, B, η) variables gives the inner product $F = \sqrt{2\pi^2\left(k_y^2 + k_z^2\right)^{-1}}\,\mathrm{diag}(k, 1, k, 1$ where diag ( ) denotes the diagonal matrix [see Eq. (2)]. Using Eq. (3) we obtain the remarkably simple results:

$$G^{+}_{max} = \max\begin{cases} q\frac{k_z}{k} - 2\bar{\nu}k^2 \\ q\frac{k_z}{k} - 2\bar{\eta}k^2 \end{cases} \tag{5}$$

for the static solutions (with max{ : denoting the maximum of the two functions), and

$$G^{+}_{max} = \max \begin{cases} q\left(\frac{1}{k}\sqrt{k_z^2 + \frac{k_x^2 k_y^2}{k^2}} - \frac{k_x k_y}{k^2}\right) - 2\bar{\nu}k^2 \\ q\left(\frac{1}{k}\sqrt{k_z^2 + \frac{k_x^2 k_y^2}{k^2}} + \frac{k_x k_y}{k^2}\right) - 2\bar{\eta}k^2 \end{cases} \tag{6}$$

for the shearing wave solutions, with k, k_x evaluated at $t = 0$.

Consider first the ideal limit of Eqs. (5) and (6), $\bar{\nu} = \bar{\eta} = 0$. We see that at all wave-numbers the shearing wave can grow faster than a static structure (or as fast at $k_x = 0$). In addition, the shearing wave growth rate has maxima at $k_x(0) = \pm k_y$, at which the growth is $q\Omega$, *i.e.,* the maximum eigenvalue of the MRI, reached when $k_y = k_x = 0$, $k_z = 1/B_{0z}\sqrt{15/16}$. Thus, in the ideal limit, the MRI can have the same growth rate, $q\Omega$, for any choice of k_y, k_z, so long as the shearing wave initial condition satisfies $k_x(0) = \pm k_y$. We note that *all* channel mode perturbations ($k_x = k_y = 0$) grow at the same rate $q\Omega$, showing that even this most basic of MRI modes can grow transiently when $k_z \neq 1/B_{0z}\sqrt{15/16}$. At all wave numbers, the initial mode structure is either purely hydrodynamic or purely magnetic. Of course, these pure modes will quickly become mixed under time-evolution due to coupling terms in Eqs. (4). Unsurprisingly, adding dissipation alters some features of this result. In particular, static waves can grow faster than shearing waves at high enough wave-numbers when $\mathrm{Pm} = \bar{\nu}/\bar{\eta} \neq 1$. Rather than embarking on a detailed analysis, we illustrate this behavior in Figure 1, showing how for perturbations with large positive k_x (*i.e.,* trailing) static structures grow more rapidly. The asymmetry in k_x is caused by the choice $Pm \ll 1$.

Inclusion of global effects. We can extend this result to situations in which aspects of the local approximation may not hold (see *e.g.,* [24]) by starting our analysis from the global MHD equations in cylindrical co-ordinates [25] and applying WKB-like approximations to obtain systems of ODEs. Motivated in part by experimentally oriented literature on low Prandtl number MRI [26], we linearize the incompressible MHD equations (with constant density ρ and pressure chosen to ensure equilibrium) about the velocity profile $\boldsymbol{u}_0 = U_{0\theta} r^{-q+1}\hat{\boldsymbol{\theta}}$ and the magnetic field profile $\boldsymbol{B}_0 = B_{0\theta} r^{2\mathrm{Rb}+1}\hat{\boldsymbol{\theta}} + B_{0z}\hat{\boldsymbol{z}}$. Non-dimensionalizing the equations and Fourier analyzing in θ and z, we obtain a system of 8 linear PDEs in r and t. These are reduced to four equations with the variable transformation, $u = u_r$, $B = B_r$, $\zeta = ik_z u_\theta - i\frac{m}{r}u_z$, $\eta = ik_z B_\theta - i\frac{m}{r}B_z$, where m and k_z are the azimuthal and vertical wave numbers.

The static wave equations are obtained in much the same way as for the local case, by inserting the WKB-like ansatz $f(r,t) \sim f(t)\, e^{ik_r r}$ and assuming $(k_r r,\, k_z r,\, m) \sim 1/\epsilon$, $(\bar{\nu},\, \bar{\eta}) \sim \epsilon^2$ to obtain a

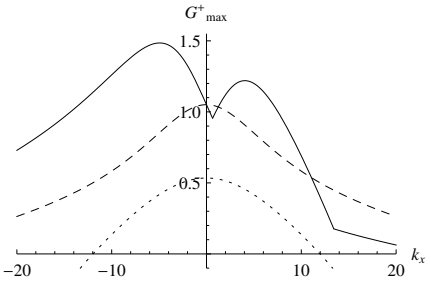

FIG. 1. G^+_{max} as a function of $k_x(0)$ for shearing waves (solid) and static solutions (dashed). The parameters are $q = 3/2$, $k_z = 5$, $k_y = 5$, $\bar{\nu} = 10^{-4}$, $\bar{\eta} = 2 \times 10^{-3}$, with the large value of $\bar{\eta}$ chosen to illustrate the dominance of static structures in for large $k_x\,(0)$. Also shown is twice the imaginary part of most unstable eigenvalue (dotted) for a vertical field $B_{0z} = 1/20$.

set of ODEs in time [27]. The shearing wave equations are obtained by assuming the solutions are predominantly waves shearing in the background flow, with an envelope that varies slowly in the r direction. To lowest order, they can be straightforwardly derived by inserting the ansatz $f(r,t) \sim f(t)\exp\left(-i\frac{m}{r}U_0 r^{-q+1}(t-t_0)\right)$ into the global equations and making the same ordering assumptions as for the static case. After non-dimensionalizing variables using the length-scale r and the time-scale $1/\Omega(r)$, one obtains

$$\partial_t U = \begin{pmatrix} -k^2\bar{\nu} - 2q\Xi\frac{mk_r}{k^2} & -2ik_z/k^2 & iF\,(r) & 2ik_z B_{az}/k^2 \\ i(q-2)k_z & -k^2\bar{\nu} & 2i(\mathrm{Rb}+1)k_z B_{az} & iF\,(r) \\ iF\,(r) & 0 & -k^2\bar{\eta} & 0 \\ -2i\mathrm{Rb}k_z B_{az} & iF\,(r) & -iqk_z & -k^2\bar{\eta} \end{pmatrix} \cdot U. \tag{7}$$

Here $U = (u, \zeta, B, \eta)$, $\Xi = 1$ or 0 for shearing waves and static waves respectively, $B_{az} = B_{0\theta} r^{2\mathrm{Rb}+1}$, $F(r) = k_z B_{0z} + mB_{az}$, wave numbers (k_r, k_z) have been scaled by r and $(\bar{\nu}, \bar{\eta})$ have been scaled by $r^2\Omega(r)$. In the static case we have substituted $\frac{\partial}{\partial t} \to \frac{\partial}{\partial t} - i\boldsymbol{u}_0 m/r$ (as for the local calculation) and for the shearing wave, $k_r = qU_0 m r^{-q}(t - t_0)$. While all variables in Eqs. (7) technically depend on both r and t, the dependence on r is parametric in keeping with WKB. The static version ($\Xi = 0$) of Eqs. (7) is very similar to the dispersion relation given in [28], aside from slight differences in how the azimuthal wavenumber m appears in the dissipation terms. Note that Eqs. (7) reduce to Eqs. (4) in the "local" limit [29].

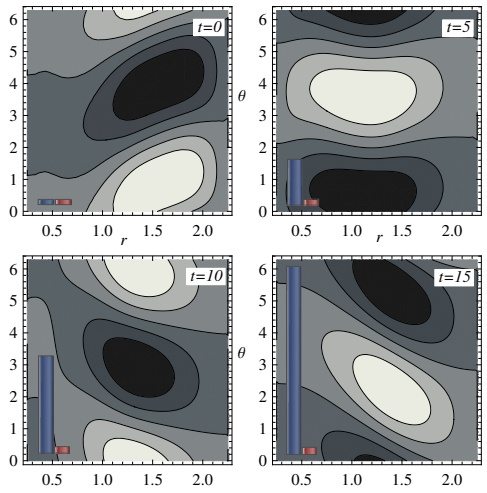

FIG. 2. Structure of the magnetic field component of the perturbation that maximizes late time energy amplification for $m = 1, k_z = 2$. Note that the perturbation shears with the background flow over the illustrated time period. The global parameters are: $U_0 = 1$, $q = 3/2$, Rb $= -1$, $B_{0z} = 0.07$, $B_{az} = 0.4$, $\bar{\nu} = 1/8000$, $\bar{\eta} = 1/50$, with the large $\bar{\eta}$ chosen to be applicable to liquid metal experiments. White and black regions show positive and negative values respectively. The bars on the left of each frame illustrate the relative energy amplification of the pictured fastest growing perturbation (blue) and the eigenmode (red) at each time.

Applying the same procedure as earlier to calculate the $t = 0^+$ growth rates leads to

$$G^+_{max} = \pm \left[\left(k^2 \left(\bar{\eta} - \bar{\nu} \right) - \Xi q \frac{k_r m}{k^2} \right)^2 + 4 B_{az} \left(1 + \mathrm{Rb} \right)^2 \frac{k_z^2}{k^2} \right]^{\frac{1}{2}} + \frac{q}{k} \sqrt{k_z^2 + \Xi \frac{m^2 k_r^2}{k^2}} - k^2 \left(\bar{\eta} + \bar{\nu} \right), \tag{8}$$

with the $\pm$ chosen to obtain the maximum value of G^+_{max}. Note that $|r\,\partial_r f|^2 \approx r^2 |\partial_r f|^2$ has been applied in the energy norm used to calculate Eq. (8), in keeping with approximations used earlier. Eq. (8) demonstrates that the fundamental results presented earlier are essentially unchanged by the addition of certain global effects, as well as illustrating the importance of shearing waves in flows with more complex shear profiles. We see that in the ideal limit (or more generally at Pm $= 1$), shearing waves always grow faster than static structures over short time-scales. The extra terms in the global equations do however change the maximum of G^+_{max} with respect to $k_x(0)$, and the MRI can grow faster than $q\Omega$ for strong $B_{0\theta}$. It is interesting that for the very large $\bar{\eta}$ characteristic of liquid metal experiments there is a large regime (for $k_x(0) > 0$) where static structures grow faster than shearing waves (see Fig. 1).

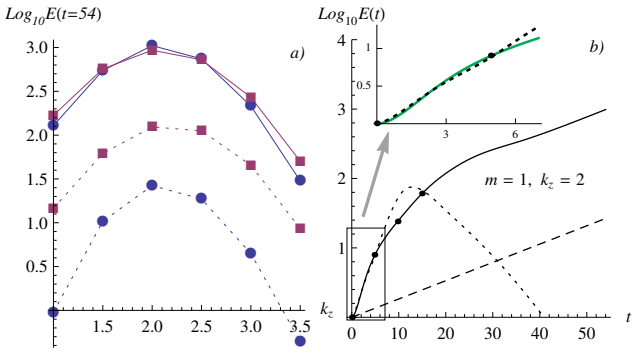

FIG. 3. *(a)* Amplification of perturbation energy by $t = 54$ as a function of vertical wavenumber k_z for axisymmetric $m = 0$ (red, squares) and non-axisymmetric $m = 1$ (blue, circles) disturbances. The solid lines illustrate the amplification of the disturbance starting from initial conditions that optimize growth at late times, the dashed lines illustrate amplification of the most unstable eigenmode. Global parameters are the same as for Fig. 2. *(b)* $E(t)$ for the optimal perturbation shown in Fig. 2 (solid), compared to $E(t)$ for the most unstable eigenmode growth (dashed). The dotted line illustrates energy of the shearing wave, obtained by solving Eqs. (7) for $r = 1.5$, $t_0 = 6$.

Transient growth and MRI saturation. While much of the motivation for this work has been related to turbulent situations, we present as a final example a simple illustration of how eigenmode predictions could be misleading in a liquid metal experiment [26, 30]. We consider the global system spanning in radius from $r = 0.25 \rightarrow 2.25$, discretize radially with Chebyshev polynomials and calculate the initial conditions that lead to the largest amplification at $t = 30$ (results are insensitive to this choice so long as it is large enough). We then evolve these optimal initial conditions, calculate the energy growth and compare this with eigenmode predictions. This example is chosen to illustrate the necessity of using nonmodal techniques to predict the relative significance of different modes, as might be relevant in studies of MRI saturation.

The example is illustrated in Figs. 2 and 3. Immediately apparent in Figure 3a is the strong difference in predicted amplification between the nonmodal and eigenmode analyses. In particular, while eigenvalues predict the dominance of axisymmetric modes, due to stronger transient effects in the non-axisymmetric case both types of mode have been amplified by approximately the same amount by the time amplification of $\sim 10^3$ is seen. The energy growth of the nonmodal structure in Fig. 2 is illustrated in Figure 3b, showing a fast initial rise followed by growth at the rate of the most unstable eigenmode. Since the transiently growing structure resembles a shearing wave (Fig. 2), for comparison we show the WKB shearing wave growth [Eqs. (7)], with $k_x(0)$ obtained through comparison to the global magnetic field structure around its peak in r. The initial conditions are obtained by maximizing the energy amplification in the same way as for the global

solution. Considering that the assumptions used to derive Eqs. (7) are far from satisfied – the wave structure varies slowly compared to r, and m is decidedly not large – the agreement is remarkably good (see inset). At larger times the shearing wave must decay due to the increasing k_r and high $\bar{\eta}$, while the global solution starts to more closely resemble the most unstable eigenmode (similar to the $t = 15$ pane in Fig. 2).

Conclusions. We have analyzed the linear MRI in the short time limit, obtaining exact results within WKB-like approximations from both local [Eqs. (5) and (6)] and global [Eqs. (8)] MHD equations. By comparing the growth of shearing waves and static structures, we prove that shearing structures always dominate in the ideal limit and that the peak growth rates are identical to those of the axisymmetric channel mode. Of course, this result contains no information about the length of time over which the short time growth can persist, and thus the overall amplification of a given mode over finite times. Indeed, since the growth rates are completely independent of magnetic field, more information is certainly needed to consider a quasi-linear mechanism for the accretion disk dynamo. Most important is probably the provision for growth over finite time-scales, as well as the effects of spatial inhomogeneity in the background fields [10]. Aside from such problems, perhaps the most suggestive idea from the results presented in this work is that turbulence in these types of magnetic shearing systems could be of a fundamentally different character than usually envisaged. In particular, since disturbances are strongly amplified *linearly* over short times at all dynamically relevant scales, the idea of a turbulent cascade and inertial range may not have the same relevance as for fluid turbulence [14]. In any case no matter how applicable such concepts might turn out to be, it seems clear that an over-reliance on eigenvalue and dispersion relation analyses can lead to incorrect growth predictions in many regimes.

We extend thanks to Dr. Jeremy Goodman for enlightening discussion. This work was supported by Max Planck/Princeton Center for Plasma Physics and U.S. DOE (DE-AC02-09CH11466).

[1] S. A. Balbus and J. F. Hawley, Astrophys. J. **376**, 214 (1991).

[2] J. F. Hawley, C. F. Gammie, and S. A. Balbus, Astrophys. J. **440**, 742 (1995).

[3] P. J. Käpylä and M. J. Korpi, Mon. Not. R. Astron. Soc. **413**, 901 (2011).

[4] J. B. Simon, K. Beckwith, and P. J. Armitage, Mon. Not. R. Astron. Soc. **422**, 2685 (2012).

[5] K. A. Sorathia, C. S. Reynolds, J. M. Stone, and K. Beckwith, Astrophys. J. **749**, 189 (2012).

[6] S. Fromang and J. Papaloizou, Astron. Astrophys. **476**, 1113 (2007).

[7] P. Y. Longaretti and G. Lesur, Astron. Astrophys. **516**, 51 (2010).

[8] E. G. Blackman, Physica Scripta **86**, 058202 (2012).

[9] M. E. Pessah, C.-k. Chan, and D. Psaltis, Phys. Rev. Lett. **97**, 221103 (2006).

[10] G. Lesur and G. I. Ogilvie, Mon. Not. R. Astron. Soc. **391**, 1437 (2008).

[11] E. T. Vishniac and A. Brandenburg, Astrophys. J. v.475 **475**, 263 (1997).

[12] T. Heinemann, J. C. McWilliams, and A. A. Schekochihin, Phys. Rev. Lett. **107**, 255004 (2011).

[13] G. Lesur and P. Y. Longaretti, Astron. Astrophys. **528**, 17 (2011).

[14] V. Bratanov, F. Jenko, D. R. Hatch, and M. Wilczek, Phys. Rev. Lett. **111**, 075001 (2013).

[15] L. N. Trefethen and M. Embree, *Spectra and Pseudospectra*, The Behavior of Nonnormal Matrices and Operators (Princeton University Press, 2005).

[16] P. J. Schmid, Annual Review of Fluid Mechanics **39**, 129 (2007).

[17] S. A. Balbus and J. F. Hawley, Astrophys. J. v.400 **400**, 610 (1992).

[18] J. C. B. Papaloizou and C. Terquem, Mon. Not. R. Astron. Soc. **287**, 771 (1997).

[19] B. M. Johnson, Astrophys. J. **660**, 1375 (2007).

[20] G. R. Mamatsashvili, G. D. Chagelishvili, G. Bodo, and P. Rossi, Mon. Not. R. Astron. Soc. **435**, 2552 (2013).

[21] Y. M. Shtemler, M. Mond, and E. Liverts, Mon. Not. R. Astron. Soc. **421**, 700 (2012).

[22] E. Knobloch, Mon. Not. R. Astron. Soc. **255**, 25P (1992).

[23] Note that the local shearing wave equations are actually nonlinearly valid due to fortuitous cancellations in Eqs. (1) upon insertion of the shearing wave ansatz.

[24] M. E. Pessah and D. Psaltis, Astrophys. J. **628**, 879 (2005).

[25] A. Bondeson, R. Iacono, and A. Bhattacharjee, Physics of Fluids **30**, 2167 (1987).

[26] G. Rüdiger, R. Hollerbach, and L. L. Kitchatinov, *Magnetic Processes in Astrophysics*, Theory, Simulations, Experiments (John Wiley & Sons, 2013).

[27] These ordering assumptions arise from assuming the solution varies faster than the background equilibrium. If either $\bar{\nu}$ or $\bar{\eta}$ are very large one may wish to alter these, leading to slightly different shearing wave equations.

[28] O. N. Kirillov and F. Stefani, Phys. Rev. Lett. **111**, 061103 (2013).

[29] O. M. Umurhan and O. Regev, Astron. Astrophys. **427**, 855 (2004).

[30] M. D. Nornberg, H. Ji, E. Schartman, A. Roach, and J. Goodman, Phys. Rev. Lett. **104**, 074501 (2010).

The Princeton Plasma Physics Laboratory is operated
by Princeton University under contract
with the U.S. Department of Energy.

Information Services
Princeton Plasma Physics Laboratory
P.O. Box 451
Princeton, NJ 08543

Phone: 609-243-2245
Fax: 609-243-2751
e-mail: pppl_info@pppl.gov
Internet Address: http://www.pppl.gov